Computer Aided Geometric Design 26 (2009) 317–335

Contents lists available at ScienceDirect

Computer Aided Geometric Design

www.elsevier.com/locate/cagd

# Using signature sequences to classify intersection curves of two quadrics

Changhe Tu [a], Wenping Wang [b,*], Bernard Mourrain [c], Jiaye Wang [a]

[a] *Shandong University*
[b] *University of Hong Kong*
[c] *INRIA*

ARTICLE INFO

*Article history:*
Received 27 July 2007
Received in revised form 21 July 2008
Accepted 6 August 2008
Available online 10 September 2008

*Keywords:*
Intersection curves
Quadric surfaces
Signature sequence
Index function
Morphology classification
Exact computation

ABSTRACT

We present a method that uses signature sequences to classify the intersection curve of two quadrics (QSIC) or, equivalently, quadric pencils in $\mathbb{PR}^3$ (3D real projective space), in terms of the shape, topological properties, and algebraic properties of the QSIC. Specifically, for a QSIC we consider its singularity, reducibility, the number of its components, and the degree of each irreducible component, etc. There are in total 35 different types of non-degenerate quadric pencils. For each of the 35 types of QSICs given by these non-degenerate pencils, through a detailed study of the eigenvalue curve and the index function jump we establish a characterizing algebraic condition expressed in terms of the Segre characteristics and the signature sequence of the quadric pencil. We show how to compute a signature sequence with rational arithmetic and use it to determine the type of the intersection curve of any two quadrics which form a non-degenerate pencil. As an example of application, we discuss how to apply our results to collision detection of cones in 3D affine space.



## 1. Introduction

### 1.1. Background

Quadric surfaces, being the simplest curved surfaces, are widely used in computational science for shape representation. It is therefore often necessary to compute the intersection or detect the interference of two quadrics. In computer graphics and CAD/CAM, the intersection curve of two quadrics needs to be found for computing a boundary representation of a 3D shape defined by quadrics. In robotics (Rimon and Boyd, 1997) and computational physics (Lin and Ng, 1995; Perram et al., 1996) one needs to perform interference analysis between ellipsoids representing or approximating the shape of various objects. There have recently been rising interests in computing the arrangements of quadric surfaces in computational geometry (Mourrain et al., 2005b; Berberich et al., 2005), a field traditionally focused on linear primitives.

The intersection curve of two quadric surfaces will be abbreviated as *QSIC*. Exact determination of the morphology of a QSIC is critical to the robust computation of its parametric description. We will mainly consider the classification of a QSIC in $\mathbb{PR}^3$ (3D real projective space) by its topological properties and algebraic properties, including singularity, the number of its components, and the degree of each irreducible component, etc. This classification is slightly finer than the morphology of the QSIC; for example, we distinguish a non-degenerate QSIC with two disconnected components from a reducible QSIC with two disconnected components being two conics, though both have the same shape structure.

* Corresponding author at: Department of Computer Science, The University of Hong Kong, Pokfulam Road, Hong Kong, China.
*E-mail address:* wenping@cs.hku.hk (W. Wang).

0167-8396/$ – see front matter © 2008 Published by Elsevier B.V.
doi:10.1016/j.cagd.2008.08.004

There are many types of QSICs in $\mathbb{PR}^3$ (Sommerville, 1947). A nonsingular QSIC can have zero, one, or two components. When a QSIC is singular, it can be either irreducible or reducible. A singular but irreducible QSIC may have three different types of singular points, i.e., acnode, cusp, and crunode. A reducible QSIC may consist of only planar components, such as lines and conics, or consist of a real line and a real space cubic curve; further distinction can be made according to whether its irreducible components are imaginary.

There are mainly three basic problems in studying the morphology of a QSIC: 1) *Enumeration*: listing all possible morphologically different types of QSICs; 2) *Classification*: determining the morphology of the QSIC of two given quadrics; 3) *Representation*: determining the transformation which brings a given QSIC into a canonical representative of its class. We emphasize on the second problem of classification, which is an algorithmic issue, while also having the first problem solved. Specifically, we enumerate all 35 different morphologies of QSIC, and characterize each of these morphologies using the signature sequence of the QSIC that can exactly be computed using rational arithmetic for the purpose of classification. The third problem, not handled here, leads to a lengthy case by case study which depends a lot on the application behind.

Consider the intersection curve of two quadrics given by $\mathcal{A}$: $X^T AX = 0$ and $\mathcal{B}$: $X^T BX = 0$, where $X = (x, y, z, w)^T \in \mathbb{PR}^3$ and $A, B$ are $4 \times 4$ real symmetric matrices. The *characteristic polynomial* of $\mathcal{A}$ and $\mathcal{B}$ is defined as

$$f(\lambda) = \det(\lambda A - B), \tag{1}$$

and $f(\lambda) = 0$ is called the *characteristic equation* of $\mathcal{A}$ and $\mathcal{B}$.

The characteristic polynomial $f(\lambda)$ is defined with a projective variable $\lambda \in \mathbb{PR}$; thus it is either a quartic polynomial or vanishes identically. For two distinct quadrics, the latter case of $f(\lambda)$ vanishing identically occurs if and only if $\mathcal{A}$ and $\mathcal{B}$ are two singular quadrics sharing a singular point or sharing a double line, that is, all the quadrics in the pencil formed by $\mathcal{A}$ and $\mathcal{B}$ are singular. In this case, the pencil of $\mathcal{A}$ and $\mathcal{B}$ is said to be *degenerate*; otherwise, the pencil is *non-degenerate*. For example, if $\mathcal{A}$ and $\mathcal{B}$ are two cones with their vertices at the same point, then they form a degenerate pencil; in this case, by projecting the two quadrics from their shared vertex to a plane $\mathbb{P}$ not passing through the center of projection, we reduce the problem of computing the QSIC to one of computing the intersection of two conics in the plane $\mathbb{P}$, which is a separate and relatively simple problem. Analyzing *degenerate* pencils can be reduced to factoring out the largest power of $u$ in $\det(\lambda A - B - uI)$ and analyzing the remaining polynomial. It is a separate and similar problem as the one we are going to describe, exploiting their normal form (Lancaster and Rodman, 2005, p. 419). For the sake of space, we will not cover the case of $f(\lambda)$ vanishing identically. Hence, we assume throughout that $f(\lambda)$ does not vanish identically.

Our contributions are the following. We consider a new characterization of the QSIC of a pencil, namely the signature sequence, and show how it can be computed effectively using only rational arithmetic operations. We establish a complete correspondence among QSIC morphologies, Segre characteristics over real numbers, Quadric Pair Canonical Forms (Muth, 1905; Williamson, 1935; Uhlig, 1976) and signature sequences. This correspondence allows us to derive a direct algorithm based on exact arithmetic for the classification of QSIC. We obtain a complete table of all the possible morphologies of QSIC, with their Segre characteristics, signature sequences and Quadric Pair Canonical Forms. Tables 1, 2 and 3 in Section 4 give the complete list of all 35 different types of QSICs in $\mathbb{PR}^3$ with non-degenerate quadric pencils. A detailed explanation of these tables is given in Section 4.3.

Note that our results are *not* about affine classification of QSICs, although the results can be used in an implementation of affine classification by further considering the intersection of a QSIC with the plane at infinity in an affine space.

The remainder of the paper is organized as follows. We discuss related work in the rest of this section. In Section 2, we present necessary preliminary concepts, such as Quadric Pair Canonical Forms. Eigenvalue curves and index sequences are introduced in Section 3. In Section 4, we present the complete list of QSICs and the algorithm for classifying the QSIC of two given quadrics. An application of our classification results to collision detection is discussed in Section 5. We conclude the paper in Section 6.

Overall, this paper is about a new algorithm for determining the type of an input QSIC based on a set of algebraic conditions (i.e., signature sequences), as previously presented in our technical report (Tu et al., 2005). Since identifying the signature sequences for all the 35 types of QSICs entails lengthy proofs, due to space limitation, we will only present the proof in two cases to explain the main idea of our approach and refer the reader to the accompanying and updated technical report (Tu et al., 2008) for the other proofs.

### *1.2. Related work*

Literature on quadrics abounds, including both classical results from algebraic geometry and modern ones from computer graphics, CAGD and computational geometry. Classifying the QSIC is a classical problem in algebraic geometry, but many solutions found therein are given in $\mathbb{PC}^3$ (3D complex projective space), and, moreover, little attention has been paid to effective computation issues. QSICs in $\mathbb{PR}^3$, real projective space, are studied comprehensively in Killing (1872), Staude (1914), but again the algorithmic aspect of classification is not considered. The topology of the zero-sets of non-degenerate real quadratic mappings in any dimension is studied in Agrachëv (1988), Agrachëv and Gamkrelidze (1989).

Some methods for computing the QSIC in computer graphics and CAGD literature do not classify the QSIC morphology completely, while others use a procedural approach to computing the QSIC morphology. The procedural approach is usually lengthy, therefore prone to erroneous classification if floating point arithmetic is used or leading to exceedingly large integer values or complicated algebraic numbers if exact arithmetic is used.

When the input quadrics are *natural quadrics*, which are special quadrics including spheres, circular right cones and cylinders, there are several methods that exploit their geometric properties to devise robust methods for computing the QSIC (Miller, 1987; Miller and Goldman, 1995; Shene and Johnstone, 1994). However, we shall consider only methods for computing the QSIC of two general quadrics and how these methods classify the QSIC morphology.

In algebraic geometry the QSIC morphology is classified in $\mathbb{PC}^3$, the complex projective space, using the Segre characteristic (Bromwich, 1906). Given two quadratical forms $A$ and $B$, the Segre characteristic is defined by the multiplicities of the roots of $f(\lambda) \equiv \det(\lambda A - B) = 0$ and the Jordan blocks associated with each multiple root with respect to the matrix $A^{-1}B$. The Segre characteristic assumes that the input quadrics are defined with complex coefficients, and therefore it does not distinguish whether a root of $f(\lambda) = 0$ is real or imaginary. When applying the Segre characteristic in $\mathbb{PR}^3$, different types of QSICs in $\mathbb{PR}^3$ may correspond to the same Segre characteristic, thus cannot be distinguished. One example is the case where four morphologically different types of nonsingular QSICs correspond to the same Segre characteristic [1111], meaning that $f(\lambda) = 0$ has four distinct roots; (see cases 1 through 4 in Table 1, Section 4.3).

A well-known method for computing QSIC in 3D real space is proposed by Levin (1976, 1979), based on the observation that there exists a ruled quadric in the pencil of any two distinct quadrics in $\mathbb{PR}^3$. Levin's method substitutes a parameterization of this ruled quadric to the equation of one of the two input quadrics to obtain a parameterization of the QSIC. However, this method does not classify the morphology of the QSIC; for instance, it does not produce a rational parameterization for a degenerate QSIC, which is always a rational curve or consists of lower-degree rational components.

Several methods have been proposed to improve Levin's method. Sarraga (1983) refines Levin's method in several aspects but does not attempt to completely classify the QSIC. Wilf and Manor (1993) combine Levin's method with the Segre characteristic to devise a hybrid method, which, however, is still not capable of completely classifying the QSIC in $\mathbb{PR}^3$; for example, the four different types of nonsingular QSICs are not classified in $\mathbb{PR}^3$. Wang et al. (2003) give procedures to classify irreducible QSICs within the framework of Levin's method, but with no systematical approach to a complete classification. Dupont et al. (2003) (see also Dupont (2004), Dupont et al. (2008a, 2008b, 2008c)) proposed a variant of Levin's method in exact arithmetic by selecting a special ruled quadric in the pencil of two quadrics, in order to minimize the number of radicals used in representing the QSIC; an implementation of this method is described in Lazard et al. (2004).

The work of Ocken et al. (1987), Dupont et al. (Dupont, 2004; Dupont et al., 2008b), Tu et al. (2002) all use simultaneous matrix diagonalization for computing or classifying the QSIC. The diagonalization procedure used by Ocken et al. is not based on any established canonical form, such as the Quadric Pair Canonical Forms (Muth, 1905; Williamson, 1935; Uhlig, 1976), and it is incomplete—it leaves some cases of QSIC morphology missing and some other cases classified incorrectly; for example, the case of a QSIC consisting of a line and a space cubic curve is missing and the cases where $f(\lambda) = 0$ has exactly two real roots or four real roots are not distinguished. The classification by Dupont et al. involves criteria such as signature and sign of deflated polynomials at specific roots of the characteristic polynomial. It is complete and leads to a procedure to determine the type of a QSIC, covering also degenerate quadric pencils.

A different idea of computing the QSIC using a procedural approach is to project a QSIC into a planar algebraic curve and analyze this projection curve to deduce the properties of the QSIC, including its morphology and parameterization. Farouki et al. (1989) project a singular QSIC to a planar quartic curve and factorize this quartic curve to determine the morphology of this singular QSIC. Wang et al. (2002) project a QSIC to a planar cubic curve using a point of the QSIC as the center of projection; this cubic curve is then analyzed to compute the morphology and parameterization of the QSIC. However, exact computation is difficult with this method, since the center of projection is computed with Levin's method.

In this paper we intend to classify the morphology of a QSIC by simple algebraic conditions, rather than by invoking a procedure to compute an equation of the QSIC. Several arguments are in favor of this algebraic treatment. Firstly, a description of the configurations of a QSIC by algebraic conditions allows us to easily introduce new parameters. For instance, by introducing the time parameter, it has direct application in collision detection problems involving moving quadrics. Secondly, it provides a computational framework to analyze the space of configurations of QSICs and the stratification induced by this classification, that is, how the different types of QSICs are related and what happens when we move across the "border" between these types. Finally, the correlation between the canonical form of pencils and the algebraic characterization can be extended to higher dimensions.

Algebraic conditions have recently been established for QSIC morphology or configuration formed by two quadrics in some special cases. The goal here is to characterize each possible morphology or configuration using a simple algebraic condition, which can be tested or evaluated easily and exactly to determine the type of an input morphology or configuration. In related topics, a simple condition in terms of the number of negative real roots of the characteristic equation $f(\lambda)$ is given by Wang et al. (2001) for the separation of two ellipsoids. Similar algebraic conditions are obtained in Wang and Krasauskas (2004) for characterizing non-degenerate configurations formed by two ellipses in 2D and ellipsoids in 3D.

As for QSICs, the Quadric Pair Canonical Form is used in Tu et al. (2002) to derive characterizing algebraic conditions for the four types of nonsingular QSICs in terms of the number of real roots of the characteristic polynomial; however, two of the four types are not distinguished, i.e., they are covered by the same condition. This pursuit of algebraic conditions is extended in our technical report (Tu et al., 2005) to cover all 35 QSICs of non-degenerate quadric pencils, which again uses the Quadric Pair Canonical Form to derive characterizing conditions in terms of signature sequences. The present paper is based on Tu et al. (2005).

## 2. Preliminaries on quadric pair canonical forms

Recall that two square symmetric matrices $C$ and $D$ are congruent if there exists a nonsingular matrix $Q$ such that $C = Q^T D Q$. When $C$ and $D$ are congruent, the quadrics $X^T C X = 0$ and $X^T D X = 0$ are related by a projective transformation.

Given two arbitrary quadrics, there is a projective transformation to simultaneously transform the two quadrics to canonical forms having the same QSIC morphology and the same root pattern of the characteristic equation. This transformation is based on the standard results on simultaneous block diagonalization of two real symmetric matrices under congruence (Muth, 1905; Williamson, 1935; Uhlig, 1976), which we will review below.

**Definition 1.** Let $A$ and $B$ be two real symmetric matrices with $A$ being nonsingular. Then $A$ and $B$ are called a *nonsingular pair of real symmetric (r.s.) matrices*.

**Definition 2.** A $k \times k$ square matrix of the form

$$M = \begin{pmatrix} \lambda & e & & \\ & \ddots & \ddots & \\ & & \ddots & e \\ & & & \lambda \end{pmatrix}_{k\times k}$$

is called a *Jordan block of type I* associated with $\lambda$ if $\lambda \in R$ and $e = 1$ for $k \geqslant 2$ or $M = (\lambda)$ with $\lambda \in R$ for $k = 1$; $M$ is called a *Jordan block of type II* associated with complex conjugated values $a \pm ib$ if

$$\lambda = \begin{pmatrix} a & -b \\ b & a \end{pmatrix} \quad a, b \in R,\ b \neq 0 \quad \text{and} \quad e = \begin{pmatrix} 1 & 0 \\ 0 & 1 \end{pmatrix},$$

for $k \geqslant 4$ or

$$M = \begin{pmatrix} a & -b \\ b & a \end{pmatrix}$$

for $k = 2$, with $a, b \in R$, $b \neq 0$.

**Definition 3.** Let $J_1, \ldots, J_k$ be all the Jordan blocks (of type I or type II) associated with the same eigenvalue $\lambda$ of a real matrix $A$. Then

$$C = C(\lambda) = \operatorname{diag}(J_1, \ldots, J_k),$$

where $\dim(J_i) \geqslant \dim(J_{i+1})$, is called the *full chain of Jordan blocks* or *full Jordan chain of length k* associated with $\lambda$.

**Definition 4.** If $\lambda_1, \ldots, \lambda_k$ are all distinct eigenvalues of a real matrix $A$, with only one being listed for each pair of complex conjugate eigenvalues, then the *real Jordan normal form* of $A$ is $J = \operatorname{diag}(C(\lambda_1), \ldots, C(\lambda_k))$.

**Theorem 1** *(Quadric Pair Canonical Form). Let $A$ and $B$ be a nonsingular pair of real symmetric matrices of size $n$. Suppose that $A^{-1}B$ has real Jordan normal form* $\operatorname{diag}(J_1, \ldots, J_r, J_{r+1}, \ldots, J_m)$*, where $J_1, \ldots, J_r$ are Jordan blocks of type I corresponding to the real eigenvalues of $A^{-1}B$ and $J_{r+1}, \ldots, J_m$ are Jordan blocks of type II corresponding to the complex eigenvalues of $A^{-1}B$. Then the following properties hold*:

(1) *$A$ and $B$ are simultaneously congruent by a real congruence transformation to*

$$\operatorname{diag}(\varepsilon_1 E_1, \ldots, \varepsilon_r E_r, E_{r+1}, \ldots, E_m)$$

*and*

$$\operatorname{diag}(\varepsilon_1 E_1 J_1, \ldots, \varepsilon_r E_r J_r, E_{r+1} J_{r+1}, \ldots, E_m J_m),$$

*respectively, where $\varepsilon_i = \pm 1$ and the $E_i$ are of the form*

$$\begin{pmatrix} 0 & \cdots & 0 & 1 \\ \vdots & \iddots & 1 & \vdots \\ 0 & 1 & \iddots & \vdots \\ 1 & 0 & \cdots & 0 \end{pmatrix}$$

*of the same size as $J_i$, $i = 1, 2, \ldots, m$. The signs of $\varepsilon_i$ are unique (up to permutations) for each set of indices $i$ that are associated with a set of identical Jordan blocks $J_i$ of type I.*

(2) *The characteristic polynomial of $A^{-1}B$ and $\det(\lambda A - B)$ have the same roots $\lambda_j$ with the same multiplicities $\gamma_i$.*

(3) *The sum of the sizes of the Jordan blocks corresponding to a real root $\lambda_i$ is the multiplicity $\gamma_i$ if $\lambda_i$ is real or twice this multiplicity if $\lambda_i$ is complex. The number of the corresponding blocks is $\rho_i = n - \operatorname{rank}(\lambda_i A - B)$, and $1 \leqslant \rho_i \leqslant \gamma_i$.*

As detailed in the review article (Lancaster and Rodman, 2005), this result about Quadric Pair Canonical Form has a long history. It was proved in Muth (1905) for non-degenerate pencils, and then further extended and rediscovered several times.

There are two transformations that can be used to simplify the analysis of the QSIC of two quadrics $\mathcal{A}$: $X^T AX = 0$ and $\mathcal{B}$: $X^T BX = 0$. Based on Quadric Pair Canonical Form, we may apply a projective transformation to both $\mathcal{A}$ and $\mathcal{B}$ to get a pair of quadrics $\mathcal{A}'$: $X^T(Q^T AQ)X = 0$ and $\mathcal{B}'$: $X^T(Q^T BQ)X = 0$ in canonical forms. The transformed quadrics $\mathcal{A}'$ and $\mathcal{B}'$ are projectively equivalent to $\mathcal{A}$ and $\mathcal{B}$, therefore have the same QSIC morphology in $\mathbb{PR}^3$ and the same characteristic equation as the pair $\mathcal{A}$ and $\mathcal{B}$.

To simplify the study of a QSIC as the base curve of the pencil spanned by two quadrics $\mathcal{A}$ and $\mathcal{B}$, we may also replace $\mathcal{A}$ and $\mathcal{B}$ by some other two distinct quadrics in the pencil, since any two distinct members of the pencil have the same QSIC as that of $\mathcal{A}$ and $\mathcal{B}$, and their characteristic polynomial is different from that of $\mathcal{A}$ and $\mathcal{B}$ only by a projective (i.e., rational linear) variable substitution, which does not alter the multiplicities of the roots of the characteristic polynomial of $\mathcal{A}$ and $\mathcal{B}$.

In order to apply Theorem 1, apparently, $A$ needs to be nonsingular. For a given pair of quadrics $A$ and $B$, if $A$ is singular, since we assume that they form a non-degenerate pencil (see Section 1), $A$ can be replaced by a nonsingular quadric $A'$ in the pencil. Then $A'$ and $B$ are a nonsingular pair of real symmetric matrices and they form the same pencil as $A$ and $B$, thus they have the same intersection curve. Note that only the existence of a nonsingular member in the pencil is required in our application of Theorem 1, and there is no need to actually compute such a nonsingular member. Hence, our results are still valid in the case where $A$ or $B$ is singular, as long as they form a non-degenerate pencil, that is, $f(\lambda)$ does not vanish identically.

## 3. Signature sequences

### 3.1. Eigenvalue curves and index sequences

**Signature and index:** Any $n \times n$ real symmetric matrix $D$ is congruent to a unique diagonal form $D' = \mathrm{diag}(I_i, -I_j, 0_k)$. The *signature*, or *inertia*, of $D$ is $(\sigma_+, \sigma_-, \sigma_0) = (i, j, k)$. The *index* of $D$ is defined as $\mathrm{index}(D) = i$, the number of positive eigenvalues of $D$.

**Index function:** The index function of a quadric pencil $\lambda A - B$ is defined as

$$\mathrm{Id}(\lambda) = \mathrm{index}(\lambda A - B), \quad \lambda \in \mathbb{PR}.$$

Since $A$ and $B$ are matrices of order 4 in our discussion, i.e., $n = 4$, we have $\mathrm{Id}(\lambda) \in \{0, 1, 2, 3, 4\}$. Note that $\mathrm{Id}(\lambda)$ has a constant value in the interval between any two consecutive real roots of $f(\lambda) = 0$. The index function may have a jump across a real root of $f(\lambda) = 0$, depending on the Jordan blocks associated with the root, as we will see below. The index function $\mathrm{Id}(\lambda)$ is also defined for $\lambda = \infty$ and $-\infty$. Clearly, $\mathrm{Id}(-\infty) + \mathrm{Id}(+\infty) = \mathrm{rank}(A)$.

**Eigenvalue curve:** We consider the real eigenvalues of the pencil $\lambda A - B$, defined by the equation

$$C(\lambda, \mu) = \det(\lambda A - B - \mu I) = 0,$$

which defines the *eigenvalue curve* in the $\lambda$–$\mu$ plane. The morphology of the QSIC of a pencil $(A, B)$ can be characterized by the geometry of the curve $\mathcal{C} : C(\lambda, \mu) = 0$. First, we note that the total degree of $C(\lambda, \mu) = 0$ is 4 and its partial degree in each of $\lambda$ and $\mu$ is also 4. Since a $4 \times 4$ symmetric matrix has 4 real eigenvalues for any $\lambda \in \mathbb{R}$, the number of real roots $C(\lambda, \mu) = 0$ in $\mu$ is 4, counted with multiplicities. Consequently, there are four $\lambda$-monotone branches of $\mathcal{C}$. For any fixed $\lambda_0 \in \mathbb{R}$, the number of points of $\mathcal{C}$ on the line $\lambda = \lambda_0$ but not on the $\lambda$-axis (i.e., $\mu \neq 0$) is the rank of the quadratic form $\lambda_0 A - B$, and the number of points of $\mathcal{C}$ above the $\lambda$-axis and the number of points of $\mathcal{C}$ below the $\lambda$-axis determine the signature of $\lambda_0 A - B$. Fig. 1 shows the eigenvalue curve of the pencil spanned by the two quadrics $(y^2 + 2xz + 1 = 0, 2yz + 1 = 0)$.

**Index sequence:** Let $\lambda_j$, $j = 1, 2, \ldots, r$, be all the distinct real roots of $f(\lambda) = 0$ in the increasing order. Let $q_k$, $k = 1, 2, \ldots, r-1$, be any real numbers separating the $\lambda_j$, i.e.,

$$-\infty < \lambda_1 < q_1 < \lambda_2 < \cdots < q_{r-1} < \lambda_r < \infty.$$

Denote $s_j = \mathrm{Id}(q_j)$, $j = 1, 2, \ldots, r-1$. Denote $s_0 = \mathrm{Id}(-\infty)$ and $s_r = \mathrm{Id}(\infty)$. Then the *index sequence* of $\mathcal{A}$ and $\mathcal{B}$ is defined as

$$\langle s_0 \uparrow s_1 \uparrow \ldots \uparrow s_{r-1} \uparrow s_r \rangle,$$

where $\uparrow$ stands for a real root, single or multiple, of $f(\lambda) = 0$.

To distinguish different types of multiplicity of a real root in place of an $\uparrow$, we use $|$ to denote a real root associated with a $1 \times 1$ Jordan block, and use $\wr$ for $p$ ($p \geqslant 2$) times in a row to denote a real root associated with a $p \times p$ Jordan block. For example, a real root with Segre characteristic [11] will be denoted by $||$ in place of an $\uparrow$ in the index sequence, and a

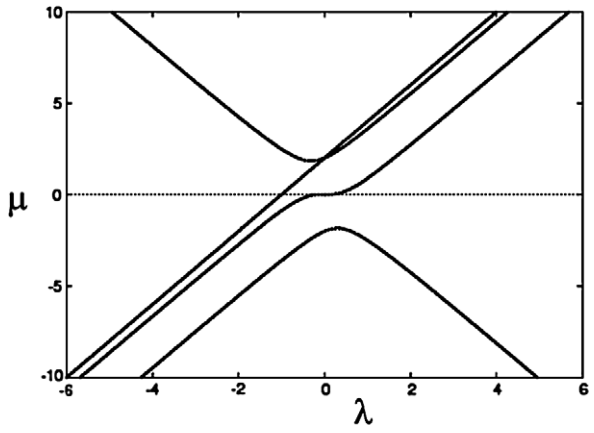


**Fig. 1.** The eigenvalue curve of the two quadrics $(y^2 + 2xz + 1 = 0, 2yz + 1 = 0)$.

real root with the Segre characteristic [21] will be denoted by $\wr\wr|$ in place of an $\uparrow$. When the Segre characteristic is (22), we use $\widehat{\wr\wr\wr\wr}$ to distinguish it from $\wr\wr\wr\wr$, which corresponds to the Segre characteristic [4]. Supposing that $\lambda_0$ is a real zero of $f(\lambda)$ with a Jordan block of size $k \times k$, we use $\wr\cdots\wr_+$ or $\wr\cdots\wr_-$ to indicate that the corresponding sign $\varepsilon_i$ of the block is $+$ or $-$.

Since $\lambda$ is a projective parameter, a projective transformation $\lambda' = (a\lambda + b)/(c\lambda + d)$, with $ad - bc \neq 0$, does not change the pencil but may change the index sequence of the pencil. Since the projective real line of $\lambda$ is a circle topologically, such a transformation induces either a rotation or a reversal of the order of the index sequence of the pencil. Therefore we need to define an equivalence relation of all index sequences of a quadric pencil under projective transformations of $\lambda$. In addition, replacing $A$ and $B$ by $-A$ and $-B$ changes each index $s_i$ to $\operatorname{rank}(\lambda A - B) - s_i$ but essentially does not change the pencil $\lambda A - B$. Note that the above replacement changes the sign associated with a Jordan block of a root; for instance, if the quadrics $\mathcal{A}$ and $\mathcal{B}$ have the index sequence $\langle 2\wr\wr_- 2|3|2\rangle$, then $-\mathcal{A}$ and $-\mathcal{B}$ have the index sequence $\langle 2\wr\wr_+ 2|1|2\rangle$.

We choose a representative in each equivalence class of index sequences such that $A$ is nonsingular; therefore, $\infty$ is not a root of $f(\lambda) = 0$ and $s_0 + s_r = 4$. Taking these observations and conventions into consideration and denoting the equivalence relation by $\sim$, this equivalence of index sequences is then defined by the following three rules:

**1) Rotation rule:**

$$\langle s_0 \uparrow s_1 \uparrow \ldots \uparrow s_{r-1} \uparrow s_r\rangle \sim \langle 4 - s_{r-1} \uparrow s_0 \uparrow s_1 \uparrow \ldots \uparrow s_{r-1}\rangle, \tag{2}$$

$$\langle s_0 \uparrow s_1 \uparrow \ldots \uparrow s_{r-1} \uparrow s_r\rangle \sim \langle s_1 \uparrow s_2 \uparrow \ldots \uparrow s_r \uparrow 4 - s_1\rangle.$$

**2) Reversal rule:**

$$\langle s_0 \uparrow s_1 \uparrow \ldots \uparrow s_{r-1} \uparrow s_r\rangle \sim \langle s_r \uparrow s_{r-1} \uparrow \ldots \uparrow s_1 \uparrow s_0\rangle. \tag{3}$$

**3) Complement rule:**

$$\langle s_0 \uparrow s_1 \uparrow \ldots \uparrow s_{r-1} \uparrow s_r\rangle \sim \langle 4 - s_0 \uparrow 4 - s_1 \uparrow \ldots \uparrow 4 - s_{r-1} \uparrow 4 - s_r\rangle. \tag{4}$$

### *3.2. Vanishing branches of eigenvalue curves*

The first goal of this paper is to tabulate the index sequences of all different quadric pencils. For this purpose we need to calculate the change of the index function, i.e., index jump, at the degenerate members of a quadric pencil $H(\lambda) = \lambda A - B$; here we just need to consider the signature variation of $H(\lambda)$ at the real zeros of $f(\lambda) = \det(H(\lambda)) = 0$. This then entails us to study the behavior of the individual branches of the eigenvalue curve $C(\lambda, \mu) = 0$ at a real root of $f(\lambda) = 0$, which are determined by the Jordan blocks of the pencil represented in Quadratic Pair Canonical Forms.

We will first show that the signature variation, i.e., the behavior of the branches of $C(\lambda, \mu) = 0$ at real zeros of $f(\lambda)$, is projectively invariant. Although this is implied by Sylvester's law of inertia, we apply Proposition 1 below, which is stronger than Sylvester's law of inertia on the invariance of the signature of a real symmetric matrix under congruence transformations. This is a new result that provides a deeper understanding of the invariance of the behavior of the eigenvalue curve's branches at a zero of $f(\lambda) = 0$ and extends the results in Agrachëv (1988), Agrachëv and Gamkrelidze (1989) to degenerate quadratic mappings.

Consider a transformation $H'(\lambda) = P^T H(\lambda) P$ of $H(\lambda)$, where $P$ is an invertible matrix. First, we compare the behavior of the eigenvalues of $H'(\lambda)$ and $H(\lambda)$. For any real symmetric matrix $Q$ of size $n$, we denote by $\rho_k(Q)$ the $k$-th real eigenvalue

of $Q$, that is, $\rho_1(Q) \leqslant \rho_2(Q) \leqslant \cdots \leqslant \rho_n(Q)$. By the Courant–Fischer Maximin Theorem (see Golub and van Loan, 1989, p. 403), we have the following inequalities:

$$\rho_k(Q)\sigma_1(P)^2 \leqslant \rho_k(P^T Q P) \leqslant \rho_k(Q)\sigma_n(P)^2, \tag{5}$$

where $\sigma_1(P)$ (resp. $\sigma_n(P)$) is the smallest (resp. largest) singular value of $P$.

**Proposition 1.** *Let $P$ be an invertible matrix and $H'(\lambda) = P^T H(\lambda) P$. If $\rho_k(H(\lambda)) = a\lambda^q(1+o(\lambda))$ with $a \neq 0, q \in \mathbb{Q}$, then $\rho_k(H'(\lambda)) = a'\lambda^q(1+o(\lambda))$ with $\operatorname{sign}(a) = \operatorname{sign}(a')$.*

**Proof.** As the eigenvalue $\rho_k(H'(\lambda))$ has a Puiseux expansion (Abhyankar, 1990; Walker, 1962) near $\lambda = 0$ of the form $\rho_k(H'(\lambda)) = \rho' + a'\lambda^{q'}(1+o(\lambda))$ with $\rho', a' \in \mathbb{R}$ and $q' \in \mathbb{Q}$, we deduce from the inequalities (5) that $\rho' = 0$, $q' = q$ and $\operatorname{sign}(a') = \operatorname{sign}(a)$. □

Proposition 1 allows us to deduce the behavior of the eigenvalues of the pencil $H(\lambda)$ from that of its Quadric Pair Canonical Form. Indeed, by Theorem 1, $H(\lambda)$ is equivalent to

$$D(\lambda) = \operatorname{diag}\big(\varepsilon_1 E_1\big(\lambda I_1 - J_1(\lambda_1)\big), \varepsilon_2 E_2\big(\lambda I_2 - J_2(\lambda_2)\big), \ldots, \varepsilon_r E_r\big(\lambda I_r - J_r(\lambda_r)\big), D'(\lambda)\big), \tag{6}$$

where $I_i$ is the identity matrix of the same size as that of the Jordan block $J_i(\lambda_i)$ of the eigenvalue $\lambda_i$, and $\det(D'(\lambda))$ has no real roots. Let $N_k(\lambda, \rho, \varepsilon) = \varepsilon E^k(\lambda I^k - J^k(\rho))$ denote a block of the preceding form of size $k \times k$. Then we have the following property:

**Proposition 2.** *The eigenvalue branch $\rho(\lambda)$ corresponding to $N_k(\lambda, \rho_0, \varepsilon)$ which vanishes at $\lambda = \rho_0$ is of the form*

$$\rho = \varepsilon \nu^k\big(1 + o(\nu)\big),$$

*where $\lambda = \rho_0 + \nu$.*

**Proof.** By an explicit expansion of the determinant $\mathcal{N}(\lambda, \mu) = \det(N_k(\lambda, \rho_0, \varepsilon) - \mu I_k)$ and denoting $\nu = \lambda - \rho_0$, we obtain

$$\mathcal{N}(\lambda, \mu) = \widetilde{\mathcal{N}}(\nu, \mu) = (-1)^k\mu^k + \cdots + (-\varepsilon)^{k-1}(-1)^{\frac{(k-1)(k-2)}{2}+1}\mu + \varepsilon^k(-1)^{\frac{k(k-1)}{2}}\nu^k.$$

The vertices of the lower envelope of the Newton polygon of $\widetilde{\mathcal{N}}(\nu, \mu)$ in the $(\mu, \nu)$-monomial space are the points $(k, 0), (1, 0), (0, k)$. By Newton's theorem (see Abhyankar, 1990, p. 89), the Puiseux expansion of the root branch which vanishes near $\rho_0$ is of the form

$$\rho = \varepsilon \nu^k\big(1 + o(\nu)\big).$$

This completes the proof. □

According to Propositions 1 and 2, if the pencil $H(\lambda)$ is equivalent to (6), then near each root $\lambda_i$, the eigenvalue branches approaching 0 are of the form $\varepsilon_i(\lambda - \lambda_i)^{k_i}(1 + o(\lambda - \lambda_i))$, where $k_i$ is the size of a block of the Quadratic Pair Canonical Form (6) of the eigenvalue $\lambda_i$ and $\varepsilon_i$ is the corresponding sign.

### 3.3. Index jump and signature sequences

The preceding analysis helps to explain how the index function $\mathrm{Id}(\lambda)$ changes its value when $\lambda$ crosses a real root of $f(\lambda) = 0$. Let $\alpha$ be a real root of $f(\lambda) = 0$. Let $\alpha_-$ and $\alpha_+$ be values sufficiently close to $\alpha$, with $\alpha_- < \alpha < \alpha_+$. Then the index jump $\Delta(\alpha)$ of $\mathrm{Id}(\lambda)$ at $\alpha$ is defined as

$$\Delta(\alpha) = \mathrm{Id}(\alpha_+) - \mathrm{Id}(\alpha_-) = \Delta^-(\alpha) + \Delta^+(\alpha),$$

where

$$\Delta^-(\alpha) = \mathrm{Id}(\alpha) - \mathrm{Id}(\alpha_-), \qquad \Delta^+(\alpha) = \mathrm{Id}(\alpha_+) - \mathrm{Id}(\alpha).$$

Suppose that the pencil $H(\lambda)$ is equivalent to (6). Let $\Delta_i^{\pm}(\alpha)$ denote the changes of signature functions of the blocks $N_{k_i}(\lambda, \lambda_i, \varepsilon_i)$ at $\alpha$. Then, we have

$$\Delta(\alpha) = \sum_{i=1}^{r} \Delta_i(\alpha), \qquad \Delta^+(\alpha) = \sum_{i=1}^{r} \Delta_i^+(\alpha), \qquad \Delta^-(\alpha) = \sum_{i=1}^{r} \Delta_i^-(\alpha). \tag{7}$$

For the index sequence $\langle s_0 \uparrow s_1 \uparrow \ldots \uparrow s_{r-1} \uparrow s_r \rangle$ of the pencil $H(\lambda) = \lambda A - B$, its corresponding *signature sequence* is defined as

$$\big\langle\big(s_0, (\cdots(p_1, n_1)\cdots), s_1, \ldots, s_{r-1}, (\cdots(p_r, n_r)\cdots), s_r\big)\big\rangle,$$

where $s_i$ is the index of $H(\lambda)$ between two consecutive real roots of $f(\lambda)=0$, $p_i$ is the number of positive eigenvalues and $n_i$ the number of negative eigenvalues at a real zero $\lambda_i$ of $f(\lambda)$. Thus, $(p_i, n_i)$ is the signature of $H(\lambda_i)$ at $\lambda_i$, and $p_i + n_i = \operatorname{rank}(\lambda_i A - B)$. The number of parentheses is the multiplicity of $\lambda_i$.

Now let us describe the signature sequence of each of $\Delta(\alpha)$, $\Delta_i^+(\alpha)$ and $\Delta_i^-(\alpha)$ separately for the cases of $k_i = 1, 2, 3, 4$. For any $a \in \mathbb{R}$, in the following we denote $a^+ = \max(a, 0)$ and $a^- = \min(a, 0)$. Note that $a^+ + a^- = a$. Furthermore, it is clear that the index jumps $\Delta(\alpha)$, $\Delta_i^+(\alpha)$ and $\Delta_i^-(\alpha)$ are zero if $\lambda_i \neq \alpha$. Therefore, we assume that $\lambda_i = \alpha$ in the following.

**(1) Jordan block of size** $1 \times 1$**:** In this case, there is one positive eigenvalue when $\lambda > \alpha$ and one negative eigenvalue when $\lambda < \alpha$. Then we have the following signature sequence $(-\varepsilon_i^-, (0,0), \varepsilon_i^+)$ and the jumps are $\Delta_i^-(\alpha) = \varepsilon_i^-$, $\Delta_i^+(\alpha) = \varepsilon_i^+$ and $\Delta_i(\alpha) = \varepsilon_i$.

**(2) Jordan block of size** $2 \times 2$**:**

$$N_{k_i}(\lambda, \alpha, \varepsilon_i) = \varepsilon_i \begin{bmatrix} 0 & \lambda - \alpha \\ \lambda - \alpha & -1 \end{bmatrix}.$$

In this case, there are two branches of the eigenvalue curve corresponding to $N_{k_i}(\lambda, \alpha, \varepsilon_i)$—one is above the $\lambda$-axis and approaches 0 when $\lambda$ approaches $\alpha$ and the other is below the $\lambda$-axis when $\lambda = \alpha$. By Proposition 2, the branch vanishing at $\alpha$ is equivalent to $\varepsilon_i(\lambda - \alpha)^2$; therefore its sign is the same before and after $\alpha$. If $\varepsilon_i > 0$, we have a positive eigenvalue branch which goes to 0 at $\alpha$; otherwise, we have a negative one. Therefore, the signature sequence of $N_{k_i}(\lambda, \alpha, \varepsilon_i)$ is $(1, ((1 - \varepsilon_i^+, 1 + \varepsilon_i^-)), 1)$ and the index jumps are $\Delta_i^-(\alpha) = -\varepsilon_i^+$, $\Delta_i^+(\alpha) = \varepsilon_i^+$ and $\Delta_i(\alpha) = 0$.

**(3) Jordan block of size** $3 \times 3$**:**

$$N_{k_i}(\lambda, \alpha, \varepsilon_i) = \varepsilon_i \begin{bmatrix} 0 & 0 & \lambda - \alpha \\ 0 & \lambda - \alpha & -1 \\ \lambda - \alpha & -1 & 0 \end{bmatrix}.$$

By Proposition 2, the vanishing eigenvalue branch is equivalent to $\varepsilon_i(\lambda - \alpha)^3$, whose sign changes before and after $\alpha$. It can be shown that, if $\varepsilon_i = 1$, the signature of $N_{k_i}(\lambda, \alpha, \varepsilon_i)$ is $(1, 2)$ when $\lambda < \alpha$ and $(2, 1)$ when $\lambda > \alpha$. If $\varepsilon_i = -1$, the signature of $N_{k_i}(\lambda, \alpha, \varepsilon_i)$ is $(2, 1)$ when $\lambda < \alpha$ and $(1, 2)$ when $\lambda > \alpha$. Thus, we have the signature sequence $(\varepsilon_i^+ - 2\varepsilon_i^-, (((1, 1))), 2\varepsilon_i^+ - \varepsilon_i^-) = (1 - \varepsilon_i^-, (((1, 1))), 1 + \varepsilon_i^+)$ and $\Delta_i^-(\alpha) = \varepsilon_i^-$, $\Delta_i^+(\alpha) = \varepsilon_i^+$ and $\Delta_i(\alpha) = \varepsilon_i$.

**(4) Jordan block of size** $4 \times 4$**:** Using a similar argument, we can show that there are two positive eigenvalues and two negative eigenvalues before and after $\alpha$ and, by Proposition 2, the eigenvalue curve approaching zero has the form $\varepsilon_i(\lambda - \alpha)^4$. Thus, the signature sequence of $N_{k_i}(\lambda, \alpha, \varepsilon_i)$ is $(2, ((((2 - \varepsilon_i^+, 2 + \varepsilon_i^-)))), 2)$ and $\Delta_i^-(\alpha) = -\varepsilon_i^+$, $\Delta_i^+(\alpha) = \varepsilon_i^+$, $\Delta_i(\alpha) = 0$.

To summarize, taking into account the sign $\varepsilon_i = \pm 1$, we have $\Delta_i(\alpha) = \varepsilon_i$ if $J_i$ has the size $1 \times 1$ or $3 \times 3$, and $\Delta_i(\alpha) = 0$ if $J_i$ has the size $2 \times 2$ or $4 \times 4$. The rank of $H(\lambda)$ drops by 1 at $\lambda = \lambda_i$ for each block of the form $N_{k_i}(\lambda, \lambda_i, \varepsilon_i)$. Thus, the signature of $H(\lambda_i)$ can be deduced directly from Jordan blocks associated with the eigenvalue $\lambda_i$ and the corresponding signs of the blocks.

### *3.4. Computation of signature sequences*

Using the signature sequence is computationally simpler than using the index sequence—we just need to compute the multiplicity of a real root and determine the signature of $\lambda A - B$ at the root; this is much simpler than determining the size of each Jordan block, as required for computing the index sequence. For a given pair of quadrics, the signature sequence is computed using only rational arithmetic as described below. Similar equivalence rules to those for index sequences apply to signature sequences as well. The signature sequences of all 35 QSIC morphologies are listed in the third column of Tables 1, 2 and 3 in Section 4.

Based on the previous analysis, it is straightforward to determine the signature sequence of the pencil $H(\lambda) = \lambda A - B$ from its Quadric Pair Canonical Form. For 30 out of the 35 cases to be considered, the signature sequence provides a unique characterization of the QSIC. The remaining 5 cases are further distinguished by their Segre characteristics. The details of this are given in Section 4.4.

Now we discuss how to use rational arithmetic to compute the signature sequence of a pair of quadrics. Consider the polynomial

$$C(\lambda, \mu) = \det(\lambda A - B - \mu I) = \mu^4 + c_3(\lambda)\mu^3 + c_2(\lambda)\mu^2 + c_1(\lambda)\mu + c_0(\lambda).$$

The values where the signature changes are defined by $C(\lambda, 0) = c_0(\lambda) = f(\lambda) = 0$. For a fixed $\lambda$, the rank of the corresponding quadratic form is the number of non-zero roots of $C(\lambda, \mu) = 0$. For any fixed $\lambda$, the number of real roots in $\mu$, counted with multiplicity, is 4. The signature of $\lambda A - B$ is determined by the rank of $\lambda A - B$ and the number of positive roots of $C(\lambda, \mu) = 0$ in $\mu$. Recall that the Descartes rule gives an exact counting of the number of positive roots if the number of real roots equals the degree of the polynomial (Basu et al., 2003). Hence, we have the following property:

**Theorem 2.** *For any $\lambda \in \mathbb{R}$,*

- *the number of positive eigenvalues of $\lambda A - B$ is the number of sign variations of* $[1, c_3(\lambda), c_2(\lambda), c_1(\lambda), c_0(\lambda)]$;
- *the number of negative eigenvalues of $\lambda A - B$ is the number of sign variations of* $[1, -c_3(\lambda), c_2(\lambda), -c_1(\lambda), c_0(\lambda)]$.

Computing the signature $\lambda A - B$ for $\lambda \in \mathbb{Q}$ is straightforward. Computing its signature at a root of $C(\lambda, 0) = f(\lambda) = 0$ can also be performed using only rational arithmetic. According to the preceding discussion, this reduces to evaluating the sign of $c_i(\lambda)$, $i = 0, 1, 2, 3$. This problem can be transformed into rational computation as follows. First, we represent a root $\alpha$ of $f(\lambda) = 0$ by

- the square-free part $p(\lambda)$ of $f(\lambda) = 0$ and
- an isolating interval $[a, b]$ with $a, b \in \mathbb{Q}$ such that $\alpha$ is the only root of $p(\lambda)$ in $[a, b]$.

Isolating intervals can be obtained efficiently in several ways (see, for instance, Mourrain et al. (2005a)). They can even be pre-computed in the case of polynomials of degree 4 (Emiris and Tsigaridas, 2003). In order to compute the sign of a polynomial $g$ at a root $\alpha$ of $f(\lambda) = 0$, we use sub-resultant (or Sturm–Habicht) sequences (Yap, 2000; Basu et al., 2003). We recall briefly the construction here and refer to Basu et al. (2003) for more details.

Given two polynomials $f(\lambda)$ and $g(\lambda) \in \mathbb{A}[\lambda]$, where $\mathbb{A}$ is the ring of coefficients, we compute the sub-resultant sequence in $\lambda$, defined in terms of the minors of the Sylvester resultant matrix of $f(\lambda)$ and $f'(\lambda)g(\lambda)$. This yields a sequence of polynomials $\mathbf{R}(\lambda) = [R_0(\lambda), R_1(\lambda), \ldots, R_N(\lambda)]$ with $R_i(\lambda) \in \mathbb{A}[\lambda]$, whose coefficients are in the same ring $\mathbb{A}$.

In our case, we take $\mathbb{A} = \mathbb{Z}$. For any $a \in \mathbb{R}$, we denote by $V_{f,g}(a)$ the number of sign variation of $\mathbf{R}(a)$. Then we have the following property (Basu et al., 2003):

**Theorem 3.**

$$V_{f,g}(a) - V_{f,g}(b) = \#\big\{\alpha \in [a, b] \text{ root of } f(\lambda) = 0 \text{ where } g(\alpha) > 0\big\} - \#\big\{\alpha \in [a, b] \text{ root of } f(\lambda) = 0 \text{ where } g(\alpha) < 0\big\}.$$

In particular, if the interval $[a, b]$ is an isolating interval for a root $\alpha$ of $c_0(\lambda) = 0$, then $V_{f,g}(a) - V_{f,g}(b)$ gives the sign of $g(\alpha)$. Taking $g(\lambda)$ to be the coefficients $c_i(\lambda)$ in Theorem 2, this method allows us to exactly compute the signature of $\alpha A - B$, using only rational arithmetic.

Efficient implementations of the algorithms presented here are available in the library SYNAPS[1] and have been applied to classifying QSIC morphologies, based on the signature sequences derived in this paper.

## 4. QSIC classification

### 4.1. Null-homotopic components and non-null-homotopic components

Topological properties are an important consideration in the classification of QSICs. We start with the definition of a loop. A loop $\mathcal{C}$ in a topological space $\mathcal{X}$ is a map from the circle $S^1$ into $\mathcal{X}$. If $\mathcal{C}$ can deform continuously into a point $p \in \mathcal{X}$, which is a constant loop, then $\mathcal{C}$ is homotopic to $p$ and is said to be *null-homotopic* (Jänich, 1984; Roseman, 1999). In our setting a real curve component $\mathcal{C}$ of a QSIC in $\mathbb{PR}^3$ is always a loop. Therefore, if there exists a plane $\mathcal{P}$ in $\mathbb{PR}^3$ such that it does not intersect $\mathcal{C}$, then $\mathcal{C}$ is a *null-homotopic* component. That is because such a component $\mathcal{C}$ appears as a bounded loop in the affine realization of $\mathbb{PR}^3$ with the plane $\mathcal{P}$ as the plane at infinity and, hence, it can deform continuously into a point. For example, a real non-degenerate conic $\mathcal{C}$ is null-homotopic in $\mathbb{PR}^3$, since it appears as an ellipse in some affine realization of $\mathbb{PR}^3$.

Refer to cases 4 and 8 in Table 1 in Section 4.3 and the corresponding illustrations in Figs. 4 and 6. It can be shown that each component of the QSIC in the two cases is a loop and has exactly one traversal intersection with the plane $w = 0$ in certain standard form (see details in the proofs in the accompanying technical report (Tu et al., 2008)). These components are *non-null-homotopic*, because a null-homotopic loop has an even number of intersections (multiplicity counted) with any plane. That is to say, these components cannot deform into a single point. The presence of non-null-homotopic components in the projective space $\mathbb{PR}^3$ is not surprising, since $\mathbb{PR}^3$ is not simply connected. Note that, although a null-homotopic component and a non-null-homotopic component are both homeomorphic to a circle, they are not of the same homotopy class. Furthermore, whether a component is null-homotopic or not is a property that is invariant under projective transformations.

### 4.2. Identifying signature sequences of all types of QSICs

We now explain the main idea of our approach to identifying the signature sequences of all types of QSICs. First, we enumerate all different Segre characteristics over the reals—this amounts to enumerating all different Quadratic Pair Canonical

[1] http://www-sop.inria.fr/galaad/software/synaps/.

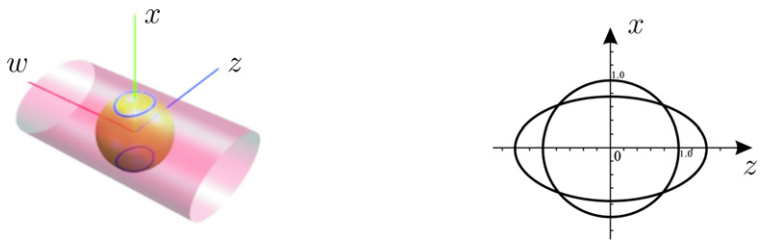


**Fig. 2.** *Left*: Intersection of the elliptic cylinder $\mathcal{B}'$ and the unit sphere $\mathcal{A}'$; *right*: the sectional view in the $z$–$x$ plane.

Forms, in terms of Jordan chains and sign combinations (see Theorem 1). Then, for each of these Quadratic Pair Canonical Forms, we find its index sequence and identify its morphology. The derivation of the index sequence is based on our preceding study on eigenvalue curves and index jumps at the real roots of the characteristics equation, while the determination of the QSIC morphology is largely a case-by-case geometric analysis of the two quadrics in their Quadric Pair Canonical Form. Finally, we convert all index sequences to their corresponding signature sequences for efficient and exact computation. In this way, we will establish a complete correspondence among the QSIC morphologies, Quadric Pair Canonical Forms and signature sequences, plus Segre characteristics.

In the following we will illustrate our approach in the simple case where the characteristic equation $f(\lambda) = 0$ has four distinct real zeros. The proofs of all the other cases can be found in the accompanying technical report (Tu et al., 2008).

**Theorem 4.** *Given two quadrics $\mathcal{A}$: $X^T AX = 0$ and $\mathcal{B}$: $X^T BX = 0$, if their characteristic equation $f(\lambda) = 0$ has four distinct real roots, then the only possible index sequences are $\langle 1|2|1|2|3\rangle$ and $\langle 0|1|2|3|4\rangle$. Furthermore,*

(1) (*Case* 1, *Table* 1) *when the index sequence is $\langle 1|2|1|2|3\rangle$, the QSIC has two null-homotopic components*;
(2) (*Case* 2, *Table* 1) *when the index sequence is $\langle 0|1|2|3|4\rangle$, the QSIC is vacuous in $\mathbb{PR}^3$.*

**Proof.** Let $\lambda_i$, $i = 1, 2, 3, 4$, denote the four distinct real roots of $f(\lambda) = 0$. By Theorem 1, $A$ and $B$ are simultaneously congruent to

$$\bar{A} = \operatorname{diag}(\varepsilon_1, \varepsilon_2, \varepsilon_3, \varepsilon_4), \quad \text{and} \quad \bar{B} = \operatorname{diag}(\varepsilon_1\lambda_1, \varepsilon_2\lambda_2, \varepsilon_3\lambda_3, \varepsilon_4\lambda_4),$$

where $\varepsilon_i = \pm 1$, $i = 1, 2, 3, 4$. Without loss of generality, we suppose that $\lambda_1 < \lambda_2 < \lambda_3 < \lambda_4$; this permutation of the diagonal elements can be achieved by a further congruence transformation to $\bar{A}$ and $\bar{B}$. Clearly, the only possible index sequences are (up to the equivalence rules described in Section 3.1) $\langle 1|2|1|2|3\rangle$ and $\langle 0|1|2|3|4\rangle$.

Recall from Section 3.3 that the index jump at a simple root (i.e., with a $1 \times 1$ Jordan block) is 1 or $-1$, depending on the sign $\varepsilon_i$ associated with the Jordan block in the Quadratic Pair Canonical Form. Hence, in order to produce the first sequence $\langle 1|2|1|2|3\rangle$, the only choices of the signs in the Quadratic Pair Canonical Forms are $\varepsilon_1 = 1, \varepsilon_2 = -1, \varepsilon_3 = 1, \varepsilon_4 = 1$. Setting $\bar{A}$ to $A'$ and $\bar{B} - \lambda_4\bar{A}$ to $B'$, we obtain

$$A' = \operatorname{diag}(1, -1, 1, 1), \qquad B' = \operatorname{diag}\big((\lambda_1 - \lambda_4), -(\lambda_2 - \lambda_4), (\lambda_3 - \lambda_4), 0\big).$$

Consider the affine realization of $\mathbb{PR}^3$ by making $y = 0$ the plane at infinity. Then $\mathcal{A}'$ is a sphere, which intersects the $x$–$z$ plane in a unit circle, while the quadric $\mathcal{B}'$ is an elliptic cylinder with the $w$-axis being its central direction, which intersects the $x$–$z$ plane in an ellipse, denoted as $\mathcal{E}$, since $\lambda_i < \lambda_4$, $i = 1, 2, 3$. It follows from the assumption $\lambda_1 < \lambda_2 < \lambda_3 < \lambda_4$ that one semi-axis of $\mathcal{E}$ is less than 1 and the other semi-axis of $\mathcal{E}$ is great than 1, shown as the configuration on the left in Fig. 2. Obviously, in this case the elliptic cylinder $\mathcal{B}'$ intersects the sphere $\mathcal{A}'$ in two disconnected null-homotopic loops.

For the second index sequence $\langle 0|1|2|3|4\rangle$, since it contains the index 0 and 4, any pencil with the index sequence $\langle 0|1|2|3|4\rangle$ contains a negative definite or positive definite quadratic form, which is an empty quadric in $\mathbb{PR}^3$. It follows that the QSIC is vacuous in this case. This completes the proof. □

### *4.3. A list of all different types of QSICs*

All the 35 different types of QSICs are listed in Tables 1, 2 and 3. In the first column are the Segre characteristics with the subscript indicating the number of real roots, not counting multiplicities. The index sequences and signature sequences are given in the second column and the third column, respectively. Here, only one representative is given for each equivalence class associated with the corresponding QSIC morphology; in several cases (cases 5, 10, and 16), there are two equivalence classes of signature sequences associated with a common QSIC morphology. The numeral label for each case, from 1 to 35, is given at the left upper corner of each entry in the second column.

Some explanations are needed for understanding the simple graphical illustration in the fourth column in Tables 1, 2 and 3. Here, a solid line or curve represents a real component and a dashed one represents an imaginary component. A solid dot indicates a real singular point, which is either isolated or the intersection of two or more components of a QSIC.

**Table 1**
Classification of QSIC that contain non-planar components in $\mathbb{PR}^3$

| $[\mathbf{Segre}]_r$ $r =$ the # of real roots | Case # Index Sequence | Signature Sequence | Illustration | Representative Quadric Pair |
|---|---|---|---|---|
| $[1111]_4$ | 1 $\langle 1\|2\|1\|2\|3\rangle$ | (1,(1,2),2,(1,2),1,(1,2),2,(2,1),3) |  | $\mathcal{A}:\ x^2+y^2+z^2-w^2=0$<br>$\mathcal{B}:\ 2x^2+4y^2-w^2=0$ |
| | 2 $\langle 0\|1\|2\|3\|4\rangle$ | (0,(0,3),1,(1,2),2,(2,1),3,(3,0),4) |  | $\mathcal{A}:\ x^2+y^2+z^2-w^2=0$<br>$\mathcal{B}:\ 2x^2+4y^2+3z^2-w^2=0$ |
| $[1111]_2$ | 3 $\langle 1\|2\|3\rangle$ | (1,(1,2),2,(2,1),3) |  | $\mathcal{A}:\ 2xy+z^2+w^2=0$<br>$\mathcal{B}:\ -x^2+y^2+z^2+2w^2=0$ |
| $[1111]_0$ | 4 $\langle 2\rangle$ | (2) |  | $\mathcal{A}:\ xy+zw=0$<br>$\mathcal{B}:\ -x^2+y^2-2z^2+zw+2w^2=0$ |
| $[211]_3$ | 5 $\langle 2\mathfrak{u}_-2\|3\|2\rangle$<br>$\langle 2\mathfrak{u}_+2\|3\|2\rangle$ | (2,((2,1)),2,(2,1),3,(2,1),2)<br>(2,((1,2)),2,(2,1),3,(2,1),2) |  | $\mathcal{A}:\ x^2-y^2+z^2+4yw=0$<br>$\mathcal{B}:\ -3x^2+y^2+z^2=0$ |
| | 6 $\langle 1\mathfrak{u}_-1\|2\|3\rangle$ | (1,((1,2)),1,(1,2),2,(2,1),3) |  | $\mathcal{A}:\ -x^2-z^2+2yw=0$<br>$\mathcal{B}:\ -3x^2+y^2-z^2=0$ |
| | 7 $\langle 1\mathfrak{u}_+1\|2\|3\rangle$ | (1,((0,3)),1,(1,2),2,(2,1),3) |  | $\mathcal{A}:\ x^2+z^2+2yw=0$<br>$\mathcal{B}:\ 3x^2+y^2+z^2=0$ |
| $[211]_1$ | 8 $\langle 2\mathfrak{u}_-2\rangle$ | (2,((2,1)),2) |  | $\mathcal{A}:\ xy+zw=0$<br>$\mathcal{B}:\ 2xy+y^2-z^2+w^2=0$ |
| $[31]_2$ | 9 $\langle 1\mathfrak{uu}_+2\|3\rangle$ | (1,(((1,2))),2,(2,1),3) |  | $\mathcal{A}:\ y^2+2xz+w^2=0$<br>$\mathcal{B}:\ 2yz+w^2=0$ |
| $[22]_2$ | 10 $\langle 2\mathfrak{u}_-2\mathfrak{u}_-2\rangle$<br>$\langle 2\mathfrak{u}_-2\mathfrak{u}_+2\rangle$ | (2,((2,1)),2,((2,1)),2)<br>(2,((2,1)),2,((1,2)),2) |  | $\mathcal{A}:\ xy+zw=0$<br>$\mathcal{B}:\ y^2+2zw+w^2=0$ |
| $[22]_0$ | 11 $\langle 2\rangle$ | (2) |  | $\mathcal{A}:\ xw+yz=0$<br>$\mathcal{B}:\ xz-yw=0$ |
| $[4]_1$ | 12 $\langle 2\mathfrak{uu}_-2\rangle$ | (2,((((2,1)))),2) |  | $\mathcal{A}:\ xw+yz=0$<br>$\mathcal{B}:\ z^2+2yw=0$ |

A null-homotopic component is drawn as a closed loop, and a non-null-homotopic component is shown as an open-ended curve.

In addition to topological properties, we also take algebraic properties into consideration in defining different types of QSICs. For example, a nonsingular QSIC may be vacuous in $\mathbb{PR}^3$, so is a QSIC consisting of two imaginary conics; these two QSICs are defined to be different, since the former is irreducible algebraically but the latter is not.

To avoid ambiguity, in the following we will also provide verbal descriptions of the simple graphics illustrations in Tables 1, 2 and 3.

#### *4.3.1. Table 1—QSICs that contain non-planar components*

**Shape descriptions of the QSICs in Table 1:**

- *Case* 1: two null-homotopic components (Fig. 3, left);
- *Case* 2: vacuous in $\mathbb{PR}^3$ (Fig. 3, right);
- *Case* 3: one null-homotopic component (Fig. 3, middle);
- *Case* 4: two non-null-homotopic components (Fig. 4);
- *Case* 5: two null-homotopic components joining at a crunode (Fig. 5, left);
- *Case* 6: one null-homotopic component and an acnode (Fig. 5, middle);
- *Case* 7: one real point, which is an acnode (Fig. 5, right);
- *Case* 8: two non-null-homotopic components intersecting at a crunode (Fig. 6);

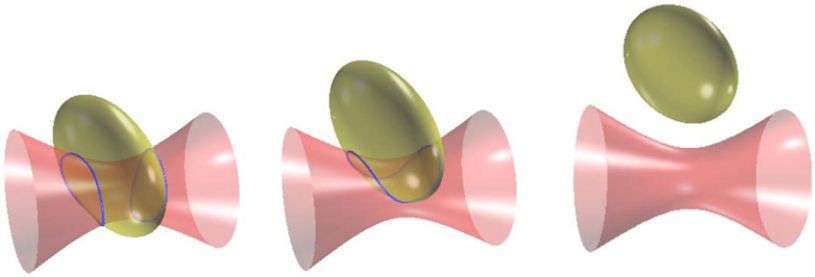

**Fig. 3.** Nonsingular QSICs. *Left*: two null-homotopic components (case 1); *middle*: one null-homotopic component (case 3); *right*: vacuous in $\mathbb{PR}^3$ (case 2).

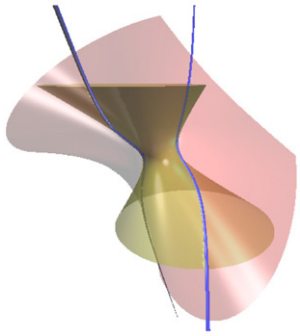

**Fig. 4.** A nonsingular QSIC with two non-null-homotopic components (case 4).

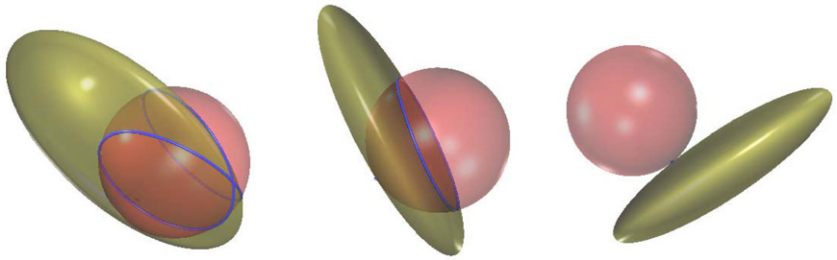

**Fig. 5.** *Left*: two null-homotopic components joining at a crunode (case 5); *middle*: one null-homotopic component and an acnode (case 6); *right*: an acnode (case 7).

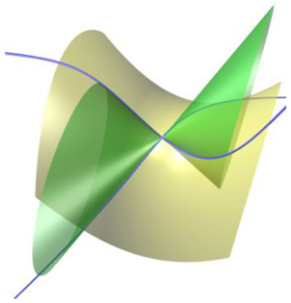

**Fig. 6.** Two non-null-homotopic components intersecting at a crunode (case 8).

- *Case* 9: one null-homotopic component having a cusp (Fig. 7);
- *Case* 10: one real line and one space cubic curve, intersecting at two distinct real points (Fig. 8, left);
- *Case* 11: one real line and one space cubic, intersecting at two complex conjugate points (Fig. 8, middle);
- *Case* 12: one real line and one real space cubic curve; the line is tangent to the cubic at a real point (Fig. 8, right).

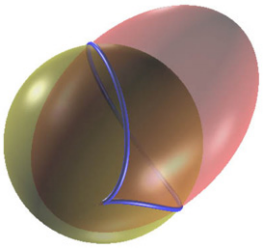

**Fig. 7.** One null-homotopic component having a cusp (case 9).

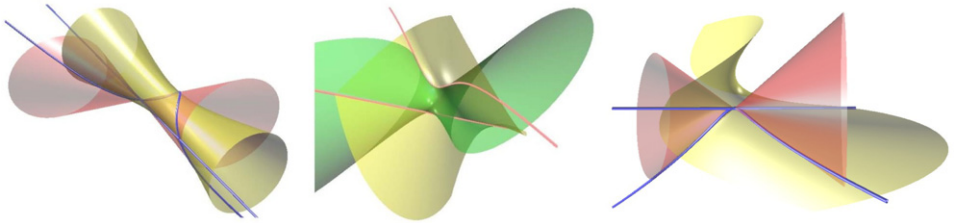

**Fig. 8.** QSICs consisting of a cubic and a real line. *Left*: the cubic and the line intersecting at two distinct real points (case 10); *middle*: the cubic and the line do not intersect at any real point (case 11); *right*: the cubic and the line are tangent at a real point (case 12).

#### 4.3.2. Table 2—QSICs with only planar components—Part I

**Shape descriptions of the QSICs in Table 2:**

- *Case* 13: two real conics intersecting at two distinct real points;
- *Case* 14: two real conics intersecting at two complex conjugate points;
- *Case* 15: two imaginary conics intersecting at two distinct real points;
- *Case* 16: two imaginary conics intersecting at two complex conjugate points;
- *Case* 17: one real conic and one imaginary conic; they intersect at two complex conjugate points;
- *Case* 18: two real conics intersecting at two distinct real points. The two conics cannot both be ellipses simultaneously in any affine realization of $\mathbb{PR}^3$. In other words, the QSIC is intersected by every plane in $\mathbb{PR}^3$;
- *Case* 19: one real conic counted twice;
- *Case* 20: one imaginary conic counted twice;
- *Case* 21: two real conics tangent to each other at one real point;
- *Case* 22: two imaginary conics tangent to each other at one real point.

#### 4.3.3. Table 3—QSICs with only planar components—Part II

**Shape descriptions of the QSICs in Table 3:**

- *Case* 23: one real conic and two real lines; they intersect pairwise at three distinct real points;
- *Case* 24: one real conic and a pair of complex conjugate lines. The conic and the pair of lines intersect at two complex conjugate points;
- *Case* 25: one imaginary conic and a pair of complex conjugate lines. The conic and the pair of lines intersect at two complex conjugate points;
- *Case* 26: one real conic and two real lines; these three components intersect at a common real point;
- *Case* 27: one real conic and a pair of complex conjugate lines; these three components intersect at a common real point;
- *Case* 28: four real lines which form a quadrangle in $\mathbb{PR}^3$;
- *Case* 29: four imaginary lines which form an imaginary quadrangle; each of the four lines intersects two of the other three at imaginary points;
- *Case* 30: two pairs of complex conjugate lines; one pair intersects the other pair at two complex conjugate points;
- *Case* 31: one pair of skew real lines and one pair of two skew imaginary lines. The two pairs of lines intersect at two pairs of complex conjugate points;
- *Case* 32: one pair of intersecting real lines, counted twice;
- *Case* 33: one pair of complex conjugate lines, counted twice;
- *Case* 34: one real double line and one pair of skew imaginary lines;
- *Case* 35: one real double line and two other skew real lines; each of the latter two lines intersects the real double line.

**Table 2**
Classification of QSIC with only planar components in $\mathbb{PR}^3$—Part I

| $[\mathbf{Segre}]_r$ $r$ = the # of real roots | Case # / Index Sequence | Signature Sequence | Illustration | Representative Quadric Pair |
|---|---|---|---|---|
| $[(11)11]_3$ | 13 $\langle 2\|\|2\|1\|2\rangle$ | (2,((1,1)),2,(1,2),1,(1,2),2) |  | $\mathcal{A}:\ x^2-y^2+z^2-w^2=0$<br>$\mathcal{B}:\ x^2-2y^2=0$ |
| | 14 $\langle 1\|\|3\|2\|3\rangle$ | (1,((1,1)),3,(2,1),2,(2,1),3) |  | $\mathcal{A}:\ -x^2+y^2+z^2+w^2=0$<br>$\mathcal{B}:\ -x^2+2y^2=0$ |
| | 15 $\langle 1\|\|1\|2\|3\rangle$ | (1,((0,2)),1,(1,2),2,(2,1),3) |  | $\mathcal{A}:\ x^2+y^2+z^2-w^2=0$<br>$\mathcal{B}:\ x^2+2y^2=0$ |
| | 16 $\langle 0\|\|2\|3\|4\rangle$<br>$\langle 1\|\|3\|4\|3\rangle$ | (0,((0,2)),2,(2,1),3,(3,0),4)<br>(1,((1,1)),3,(3,0),4,(3,0),3) |  | $\mathcal{A}:\ x^2+y^2-z^2-w^2=0$<br>$\mathcal{B}:\ x^2+2y^2=0$ |
| $[(11)11]_1$ | 17 $\langle 1\|\|3\rangle$ | (1,((1,1)),3) |  | $\mathcal{A}:\ x^2+y^2+2zw=0$<br>$\mathcal{B}:\ -z^2+w^2+2zw=0$ |
| | 18 $\langle 2\|\|2\rangle$ | (2,((1,1)),2) | 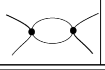 | $\mathcal{A}:\ x^2-y^2-2zw=0$<br>$\mathcal{B}:\ -z^2+w^2+2zw=0$ |
| $[(111)1]_2$ | 19 $\langle 1\|\|\|2\|3\rangle$ | (1,(((0,1))),2,(2,1),3) |  | $\mathcal{A}:\ y^2+z^2-w^2=0$<br>$\mathcal{B}:\ x^2=0$ |
| | 20 $\langle 0\|\|\|3\|4\rangle$ | (0,(((0,1))),3,(3,0),4) |  | $\mathcal{A}:\ y^2+z^2+w^2=0$<br>$\mathcal{B}:\ x^2=0$ |
| $[(21)1]_2$ | 21 $\langle 1\wr_-\|2\|3\rangle$ | (1,(((1,1))),2,(2,1),3) |  | $\mathcal{A}:\ y^2-z^2+2zw=0$<br>$\mathcal{B}:\ -x^2+z^2=0$ |
| | 22 $\langle 1\wr_+\|2\|3\rangle$ | (1,(((0,2))),2,(2,1),3) |  | $\mathcal{A}:\ y^2-z^2+2zw=0$<br>$\mathcal{B}:\ x^2+z^2=0$ |

### *4.4. Classification algorithm*

It follows from the classification theorems by Tu et al. (2005) or Tu et al. (2008) that all the conditions (i.e., signature sequences plus Segre characteristics) are necessary and sufficient for the corresponding QSIC morphologies. Hence, we can use these conditions to classify the QSIC of a given pair of quadrics in $\mathbb{PR}^3$, by computing their signature sequence derived from their index sequence (see Section 3.2).

Note that not all the signature sequences of the 35 different types of QSICs are distinct: the three different QSICs with the Segre characteristics $[1111]_0$, $[22]_0$ and $[(11)(11)]_0$ in cases 4, 11 and 31 share the same index sequence $\langle 2\rangle$, thus leading to the same signature sequence (2). Furthermore, the two different index sequences $\langle 2\wr\wr_-|2\rangle$ and $\langle 2\wr_-\wr_+2\rangle$ in cases 26 and 35 correspond to the same signature sequence (2((((1, 1))))2). Thus, in total, there are only 32 distinct signature sequences. In the following we explain how to distinguish these cases with identical signature sequences using their minimal polynomials. Recall that the minimal polynomial of a squared matrix $A$ is the polynomial $p(x)$ of the lowest degree such that $p(A)=0$ (Horn and Johnson, 1985).

Suppose that the signature sequence of an input quadric pencil has been found to be (2). We need to find out to which of cases 4, 11, and 31 the pencil belongs. In this case $f(\lambda)=0$ has no real root. Case 4 with the Segre characteristics $[1111]_0$

**Table 3**
Classification of QSIC with only planar components in $\mathbb{PR}^3$—Part II

| $[\mathbf{Segre}]_r$ $r =$ the # of real roots | Case # **Index Sequence** | **Signature Sequence** | **Illustration** | **Representative Quadric Pair** |
|---|---|---|---|---|
| $[2(11)]_2$ | 23 $\langle 2\wr\!\wr\_2 \| 2\rangle$ | (2,((2,1)),2,((1,1)),2) |  | $\mathcal{A}:\ 2xy - y^2 = 0$<br>$\mathcal{B}:\ y^2 + z^2 - w^2 = 0$ |
| | 24 $\langle 1\wr\!\wr\_1 \| 3\rangle$ | (1,((1,2)),1,((1,1)),3) |  | $\mathcal{A}:\ 2xy - y^2 = 0$<br>$\mathcal{B}:\ y^2 - z^2 - w^2 = 0$ |
| | 25 $\langle 1\wr\!\wr_+1 \| 3\rangle$ | (1,((0,3)),1,((1,1)),3) |  | $\mathcal{A}:\ 2xy - y^2 = 0$<br>$\mathcal{B}:\ y^2 + z^2 + w^2 = 0$ |
| $[(31)]_1$ | 26 $\langle 2\wr\!\wr\!\wr\_ \| 2\rangle$ | (2,((((1,1)))),2) |  | $\mathcal{A}:\ y^2 + 2xz - w^2 = 0$<br>$\mathcal{B}:\ yz = 0$ |
| | 27 $\langle 1\wr\!\wr\!\wr_+ \| 3\rangle$ | (1,((((1,1)))),3) |  | $\mathcal{A}:\ y^2 + 2xz + w^2 = 0$<br>$\mathcal{B}:\ yz = 0$ |
| $[(11)(11)]_2$ | 28 $\langle 2 \| 2 \| 2\rangle$ | (2,((1,1)),2,((1,1)),2) |  | $\mathcal{A}:\ x^2 - y^2 = 0$<br>$\mathcal{B}:\ z^2 - w^2 = 0$ |
| | 29 $\langle 0 \| 2 \| 4\rangle$ | (0,((0,2)),2,((2,0)),4) |  | $\mathcal{A}:\ x^2 + y^2 = 0$<br>$\mathcal{B}:\ z^2 + w^2 = 0$ |
| | 30 $\langle 1 \| 1 \| 3\rangle$ | (1,((0,2)),1,((1,1)),3) |  | $\mathcal{A}:\ x^2 + y^2 = 0$<br>$\mathcal{B}:\ z^2 - w^2 = 0$ |
| $[(11)(11)]_0$ | 31 $\langle 2\rangle$ | (2) |  | $\mathcal{A}:\ xy + zw = 0$<br>$\mathcal{B}:\ -x^2 + y^2 - z^2 + w^2 = 0$ |
| $[(211)]_1$ | 32 $\langle 2\wr\!\wr\_ \| 2\rangle$ | (2,((((1,0)))),2) |  | $\mathcal{A}:\ x^2 - y^2 + 2zw = 0$<br>$\mathcal{B}:\ z^2 = 0$ |
| | 33 $\langle 1\wr\!\wr\_ \| 3\rangle$ | (1,((((1,0)))),3) |  | $\mathcal{A}:\ x^2 + y^2 + 2zw = 0$<br>$\mathcal{B}:\ z^2 = 0$ |
| $[(22)]_1$ | 34 $\langle 2\widehat{\wr\!\wr}\_\widehat{\wr\!\wr}\_2\rangle$ | (2,((((2,0)))),2) |  | $\mathcal{A}:\ xy + zw = 0$<br>$\mathcal{B}:\ y^2 + w^2 = 0$ |
| | 35 $\langle 2\widehat{\wr\!\wr}\_\widehat{\wr\!\wr}_+2\rangle$ | (2,((((1,1)))),2) |  | $\mathcal{A}:\ xy - zw = 0$<br>$\mathcal{B}:\ y^2 - w^2 = 0$ |

can be identified by the fact that $f(\lambda) = 0$ has no multiple roots. This can be detected by whether the discriminant of $f(\lambda)$ vanishes, i.e., whether $\mathrm{Disc}(f) \equiv \mathrm{Res}_\lambda(f, \partial_\lambda f) = 0$.

Then case 11 with $[22]_0$ and case 31 with $[(11)(11)]_0$ are distinguished by that they have different minimal polynomials. Suppose that the input quadrics are given in the real symmetric matrices $A$ and $B$; and, without loss of generality, assume that $A$ is nonsingular. Since $f(\lambda)$ is a squared polynomial in the case of $[22]_0$ or $[(11)(11)]_0$, we write

$$f(\lambda) = (a\lambda^2 + b\lambda + c)^2,$$

whose square-free part is

$$g(\lambda) = a\lambda^2 + b\lambda + c,$$

where $a, b, c \in \mathbb{R}$ and $b^2 - 4ac < 0$. Then, by Theorem 1 and the Cauchy–Cayley Theorem, the case of $[(11)(11)]_0$ occurs if $g(\lambda)$ annihilates $A^{-1}B$, i.e., $g(A^{-1}B) = 0$; otherwise, the case of $[22]_0$ occurs. Note that $g(\lambda)$ can be obtained as the GCD of $f(\lambda)$ and $f'(\lambda)$.

Next we consider how to distinguish case 26 and case 35, whose index sequences $\langle 2\wr\wr\_|2\rangle$ and $\langle 2\wr\_\wr_+2\rangle$ are mapped to the same signature sequence $(2((((1,1))))2)$. For either of the two cases, $f(\lambda) = (\lambda - a)^4$ for some $a \in \mathbb{R}$, but the minimal polynomial is $g(\lambda) = (\lambda - a)^2$ in the case of $\langle 2\wr\_\wr_+2\rangle$, while the minimal polynomial is $h(\lambda) = (\lambda - a)^3$ in the case of $\langle 2\wr\wr\_|2\rangle$. Therefore, the case of $\langle 2\wr\_\wr_+2\rangle$ occurs if $A^{-1}B$ is annihilated by $g(\lambda)$, i.e., $g(A^{-1}B) = 0$; otherwise, the case of $\langle 2\wr\wr\_|2\rangle$ occurs. Note that $g(\lambda) = (\lambda - a)^2$ can be obtained without solving for the root $a$.

Combining the preceding methods based on minimal polynomials with the methods described in Section 3.4 for exact computation of the signature sequences, we have the following complete algorithm for exact classification of QSICs.

**Algorithm 1** *(Classification of a pair of quadrics).*
INPUT: $Q_1, Q_2 \in \mathbb{Q}[x, y, z]$ *of degree* 2.
OUTPUT: *The normal form of the shape of the intersection curve as listed in Tables 1, 2 and 3.*

- Compute the $4 \times 4$ symmetric matrices $A, B$ associated to the quadratic forms $Q_1, Q_2$.
- Compute the coefficients $c_0(\lambda), \ldots, c_3(\lambda)$ of the characteristic polynomial $C(\lambda, \mu) = \det(\lambda A - B - \mu\,\mathrm{Id}) = c_0(\lambda) + c_1(\lambda)\mu + c_2(\lambda)\mu^2 + c_3(\lambda)\mu^3 + \mu^4$.
- If $c_0(\lambda) \equiv 0$, then output "degenerate pencil".
- Isolate the real roots $\lambda_1, \ldots, \lambda_r$ of $f(\lambda) = c_0(\lambda)$ and compute their multiplicities.
- Deduce a sequence of rational numbers $q_1, \ldots, q_{r-1} \in \mathbb{Q}$ such that $\lambda_1 < q_1 < \lambda_2 < q_2 < \cdots < q_{r-1} < \lambda_r$.
- Compute the number of sign changes of $c_0(\lambda), \ldots, c_3(\lambda), 1$ at $\lambda = -\infty, q_1, \ldots, q_{r-1}$ to get the value of the index function at these points.
- Compute the sign of $c_1(\lambda), \ldots, c_3(\lambda), 1$ at $\lambda = \lambda_1, \ldots, \lambda_r$ using static Sturm Sequence (Emiris and Tsigaridas, 2003), in order to get the value of the signature at these roots.
- Construct the corresponding signature sequence.
- If the signature sequence is (2), compute $\rho = \mathrm{Res}_\lambda(f, \partial_\lambda f)$.
  - If $\rho \neq 0$, output case (4);
  - else compute $g(\lambda) \in \mathbb{Q}[\lambda]$ such that $f = g^2$ and $C = g(A^{-1}B)$.
    If $C \neq 0$, output case (11);
    otherwise output case (31);
- If the signature sequence is $(2, (((1,1))), 2)$, compute $g(\lambda) \in \mathbb{Q}[\lambda]$ such that $f = g^2$ and $C = g(A^{-1}B)$.
  - If $C \neq 0$, output case (26);
  - otherwise, output case (35);
- In the remaining cases, up to the equivalence class defined by cyclic permutation, inversion and complementary operations, the signature sequence is matched with exactly one of the signature sequences in Tables 1, 2 or 3. Look up in Tables 1, 2, 3 and output the corresponding case.

In the following we will use a working example to illustrate how our classification algorithm works

**Example 1.** Consider two quadrics

$$\mathcal{A}: \quad 20x^2 - 12xy + 48xz + 76x + 16y^2 - 16yz - 12y + 42z^2 + 72z + 58 = 0,$$

$$\mathcal{B}: \quad 28x^2 + 16xy + 80xz + 56x + 2y^2 + 24yz + 20y + 56z^2 + 72z + 14 = 0.$$

The equation of the eigenvalue curve $\mathcal{C}$ is

$$u^4 + (-136\lambda + 100)u^3 + (-1048 - 3612\lambda + 2904\lambda^2)u^2 + (-10000\lambda^3 + 22616\lambda^2 + 28416\lambda)u$$
$$- 170528\lambda^2 + 170528\lambda^3 - 85264\lambda^4 = 0.$$

Substituting $u = 0$ in this polynomial yields

$$-85264\lambda^4 + 170528\lambda^3 - 170528\lambda^2 = 0,$$

whose only real root is the double root $\lambda = 0$. Substituting $\lambda = -1$ in the equation of $\mathcal{C}$ yields

$$u^4 + 236u^3 + 5468u^2 + 4200u - 426320,$$

which has one sign change in its coefficients; therefore, by the Descartes rule, it has only one positive root. It follows that the signature sequence is $(1, ((1,1)), 3)$, which matches case 17 in Table 2. Hence, this QSIC consists of a real conic and an imaginary one.

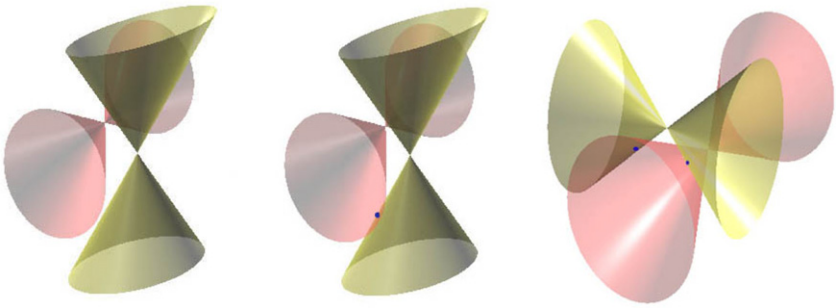

**Fig. 9.** Separation, one-point tangency and two-point tangency between two cones.

## 5. Application to collision detection

In this section, as an application to collision detection, we present a method for determining if two cones $X^T AX = 0$ and $X^T BX = 0$ are separated (that is, free of collision) in 3D affine space $\mathbb{R}^3$, using the classification results in this paper. Assume that $\mathbb{R}^3$ is obtained by treating $w = 0$ as the ideal plane, where $w$ is the last component in $X^T = (x, y, z, w)$. Without loss of generality, suppose that the signature of both $A$ and $B$ is $(\sigma_+, \sigma_-, \sigma_0) = (2, 1, 1)$, i.e., both have two positive eigenvalues, one negative eigenvalue, and one zero eigenvalue. For brevity, denote their signature by $(\sigma_+, \sigma_-) = (2, 1)$, omitting the zero eigenvalue. Then, given the matrix pencil $F(\lambda) = \lambda A - B$, the signature of $F(0)$ is $(1, 2)$ and that of $F(+\infty) = (2, 1)$.

To obtain the separation condition, first we check if the pencil is degenerate. If so, then the two cones intersect in a line containing the vertices of the two cones (see e.g. Lancaster and Rodman, 2005, p. 419). Next, if $\det(A - \lambda B) \not\equiv 0$, we look among the 35 cases in Tables 1–3 for those whose signature sequences contain the signatures $(1, 2)$ and $(2, 1)$, and the corresponding QSICs are vacuous in $\mathbb{PR}^3$, the 3D real projective space. Clearly, case 2 is the only match, with the signature sequence $(0, (0, 3), 1, (1, 2), 2, (2, 1), 3, (3, 0), 4)$. For normalization we need to assign the signature $(2, 1)$ to the root $\lambda = \infty$ and assign the signature $(1, 2)$ to the root $\lambda = 0$. Therefore, in the following we suppose that the rightmost signature corresponds to $\lambda = +\infty$ and the signature over-lined corresponds to $\lambda = 0$. Then we have the following results.

**Lemma 1.** *Two cones $X^T AX = 0$ and $X^T BX = 0$ do not intersect in $\mathbb{PR}^3$ if and only if their signature sequence is* $(1, (0, 3), 0, (0, 3), 1, \overline{(1, 2)}, 2, (2, 1))$.

Two cones may be externally tangent to each other at one or two points. One-point tangency corresponds to case 7. Therefore, by a similar argument, we have

**Lemma 2.** *Two cones $X^T AX = 0$ and $X^T BX = 0$ are externally tangent at exactly one point in $\mathbb{PR}^3$ if and only if their signature sequence is* $(1, ((0, 3)), 1, \overline{(1, 2)}, 2, (2, 1))$.

For two-point tangency, which corresponds to case 15, we have

**Lemma 3.** *Two cones $X^T AX = 0$ and $X^T BX = 0$ are externally tangent at two points in $\mathbb{PR}^3$ if and only if their signature sequence is* $(1, ((0, 2)), 1, \overline{(1, 2)}, 2, (2, 1))$.

The three cases of separation, one-point tangency and two-point tangency of two cones are illustrated in Fig. 9.

Based on Lemmas 1 through 3, we have the following procedure for determining if two input cones are separate in the affine space $\mathbb{R}^3$. Given two cones $\mathcal{A}$: $X^T AX = 0$ and $\mathcal{B}$: $X^T BX = 0$, first compute its signature sequence following Section 3.4. Then $\mathcal{A}$ and $\mathcal{B}$ are separated in $\mathbb{R}^3$ if (a) their signature sequence is the same as the one in Lemma 1; or (b) it equals to either of the sequences in Lemmas 2 and 3, and all tangent points of $\mathcal{A}$ and $\mathcal{B}$ are at infinity, i.e., lying on the plane $w = 0$. Here, for one-point tangency case, the tangent point is given by the eigenvector associated with the (rational) double roots of $f(\lambda) \equiv |\lambda A - B| = 0$. In the two-point tangency case, there is a 2-dimensional eigenspace associated with the double root of $f(\lambda) = 0$, representing a line passing though the two tangent points of the two cones. So the two tangent points can be computed by intersecting this line with either of $\mathcal{A}$ and $\mathcal{B}$. These two cases can also be analyzed by taking the homogeneous part of degree 2 of the two polynomials and check the intersection of the two plane conics at infinity, using the 2D classification of pencil of conics.

## 6. Conclusions

To summarize, we have obtained the following result:

**Theorem 5.** *There are in total* 35 *different types of QSICs with non-degenerate pencils. Each type of QSIC of a pencil* $(A, B)$ *is entirely classified by the signature sequence and the degree of the minimal polynomial of the pencil, which can be computed using only rational arithmetic.*

Besides determining the QSIC morphology for enhancing robust computation of QSIC in surface boundary evaluation, our results can also be applied to deriving simple algebraic conditions for interference analysis of quadrics. For arrangement computation, it is an interesting problem to classify all possible partitions of $\mathbb{R}^3$ that can be formed by two ellipsoids. It is also possible to apply the results here to derive efficient algebraic conditions for collision detection between various types of quadric surfaces, such as cones and cylinders, following the framework in Wang and Krasauskas (2004).

One could also use the idea developed here to study the classification of a pencil of conics in $\mathbb{PR}^2$, which facilitates the classification of QSIC of degenerate pencils in $\mathbb{PR}^3$. A more challenging problem is to use the signature sequence to classify the intersection of two quadrics in higher dimensions, $\mathbb{PR}^4$ say. Here the difficult issue is to deduce the geometry of the QSIC associated with each possible Quadric Pair Canonical Form, while it is should be straightforward to obtain the signature sequence of each normal form.

Another direction of investigation is the classification of the net of three quadrics in $\mathbb{PR}^n$. In this case, given three quadratic forms $A$, $B$ and $C$, the problem is how to use the invariants of the planar curve $f(\alpha, \beta, \gamma) \equiv \det(\alpha A + \beta B + \gamma C) = 0$ to characterize the geometric properties of the net $X^T(\alpha A + \beta B + \gamma C)X = 0$ or the intersection of the three quadrics $X^T AX = 0$, $X^T BX = 0$ and $X^T CX = 0$.

## Acknowledgements

The authors would like to thank the reviewers for their invaluable comments. The work of Changhe Tu was partially supported by the National Natural Science Foundation of China (60473127). The work of Wenping Wang was partially supported by the National Key Basic Research Project of China (2004CB318000) and the Research Grant Council of Hong Kong (HKU7178/06E).

## References

Abhyankar, S., 1990. Algebraic Geometry for Scientists and Engineers. American Mathematical Society, Providence, RI.
Agrachëv, A., 1988. Homology of intersections of real quadrics. Dokl. Akad. Nauk SSSR 299, 493–496.
Agrachëv, A., Gamkrelidze, R., 1989. Quadratic mappings and smooth vector functions: Euler characteristics of the level surfaces. In: Current Problems in Mathematics. Newest results, vol. 35 (Russian), pp. 179–239. Translated in: J. Soviet Math. 55 (4) (1991) 1892–1928.
Basu, S., Pollack, R., Roy, M.-F., 2003. Algorithms in Real Algebraic Geometry. Springer-Verlag, Berlin.
Berberich, E., Hemmer, M., Kettner, L., Schömer, E., Wolpert, N., 2005. An exact, complete and efficient implementation for computing planar maps of quadric intersection curves. In: Proc. of ACM Symposium on Computational Geometry 2005, pp. 99–106.
Bromwich, T., 1906. Quadratic Forms and Their Classification by Means of Invariant-Factors. Cambridge Tracts in Mathematics and Mathematical Physics, vol. 3.
Dupont, L., 2004. Paramétrage quasi-optimal de l'intersection de deux quadriques : théorie, algorithme et implantation. Ph.D. thesis, Thèse d'université, Université Nancy II.
Dupont, L., Lazard, D., Lazard, S., Petitjean, S., 2003. Near optimal parameterization of the intersection of quadrics. In: Proc. of the Nineteenth Annual Symposium on Computational Geometry, pp. 246–255.
Dupont, L., Lazard, D., Lazard, S., Petitjean, S., 2008a. Near-optimal parameterization of the intersection of quadrics: I. The generic algorithm. J. Symbolic Comput. 3 (43), 168–191. Rapport de Recherche INRIA 5667, 2005.
Dupont, L., Lazard, D., Lazard, S., Petitjean, S., 2008b. Near-optimal parameterization of the intersection of quadrics: II. A classification of pencils. J. Symbolic Comput. 3 (43), 192–215. Rapport de Recherche INRIA 5668, 2005.
Dupont, L., Lazard, D., Lazard, S., Petitjean, S., 2008c. Near-optimal parameterization of the intersection of quadrics: III. Parameterizing singular intersections. J. Symbolic Comput. 3 (43), 216–232. Rapport de Recherche INRIA 5669, 2005.
Emiris, I., Tsigaridas, E.P., 2003. Computing with real algebraic numbers of small degree. In: Proc. of ESA. Springer-Verlag, Berlin.
Farouki, R., Neff, C., O'Connor, M., 1989. Automatic parsing of degenerate quadric-surface intersections. ACM Trans. Graph. 8, 174–203.
Golub, G.H., van Loan, C.F., 1989. Matrix Computation, second ed. Johns Hopkins University Press, Baltimore, MD.
Horn, R.A., Johnson, C.R., 1985. Matrix Analysis. Cambridge University Press.
Jänich, K., 1984. Topology. Springer-Verlag.
Killing, W., 1872. Der Flächenbüschel Zweiter Ordnung. Gustav Schade, Berlin.
Lancaster, P., Rodman, L., 2005. Canonical forms for Hermitian matrix pairs under strict equivalence and congruence. SIAM Rev. 47 (3), 407–443.
Lazard, S., Naranda, L.P., Petitjean, S., 2004. Intersecting quadrics: an efficient and exact implementation. In: Proc. of ACM Symposium on Computational Geometry, pp. 419–428.
Levin, J., 1976. A parametric algorithm for drawing pictures of solid objects composed of quadrics. Comm. ACM 10, 555–563.
Levin, J., 1979. Mathematical models for determining the intersection of quadric surfaces. Comput. Graph. Image Process. 57, 73–87.
Lin, X., Ng, T., 1995. Contact detection algorithms for three-dimensional ellipsoids in discrete element modeling. Int. J. Numer. Anal. Methods Geomech. 19, 653–659.
Miller, J., 1987. Geometric approaches to nonplanar quadric surface intersection curves. ACM Trans. Graph. 6, 274–307.
Miller, J., Goldman, R., 1995. Geometric algorithms for detecting and calculating all conic sections in the intersection of any two natural quadric surfaces. Graph. Models Image Process. 57, 55–66.
Mourrain, B., Rouillier, F., Roy, M.-F., 2005a. Bernstein's basis and real root isolation. In: Goodman, J.J.E., Welzl, E. (Eds.), Combinatorial and Computational Geometry. In: Mathematical Sciences Research Institute Publications. Cambridge University Press.
Mourrain, B., Técourt, J., Teillaud, M., 2005b. On the computation of an arrangement of quadrics in 3D. Comput. Geom. 30, 145–164.
Muth, P., 1905. Über reelle Äquivalenz von Scharen reeller quadratischer Formen. Crelle's J. 128, 302–343.
Ocken, S., Schwartz, J.T., Sharir, M., 1987. Precise implementation of CAD primitives using rational parametrizations of standard surfaces. In: Planning, Geometry, and Complexity of Robot Motion. Ablex Publishing Corporation.

Perram, J., Rasmussen, J., Prastaard, E., Lebowitz, J., 1996. Ellipsoids contact potential: theory and relation to overlap potentials. Phys. Rev. 6, 6565–6572.
Rimon, E., Boyd, S., 1997. Obstacle collision detection using best ellipsoid fit. J. Intelligent Robotic Syst. 18, 105–126.
Roseman, D., 1999. Elementary Topology. Prentice-Hall, Inc.
Sarraga, R., 1983. Algebraic methods for intersections of quadric surfaces in GMSOLID. Comput. Vis. Graph. Image Process. 2, 222–238.
Shene, C., Johnstone, J., 1994. On the lower degree intersections of two natural quadrics. ACM Trans. Graph. 4, 400–424.
Sommerville, D., 1947. Analytical Geometry of Three Dimensions. Cambridge University Press.
Staude, O., 1914. Flächen 2. Ordnung und ihre Systeme und Durchdringungskurven. In: Meyer, W.F., Mohrmann, H. (Eds.), Encyklopädie der Mathematischen Wissenschaften, vol. III.C.2. B. G. Teubner, Leipzig, pp. 161–256.
Tu, C., Wang, W., Mourrain, B., Wang, J., 2005. Signature sequence of intersection curve of two quadrics for exact morphological classification. Tech. Rep. TR-2005-9, Department of Computer Science, The University of Hong Kong.
Tu, C., Wang, W., Mourrain, B., Wang, J., 2008. Using signature sequences to classify intersection curves of two quadrics. Tech. Rep. TR-2008-15, Department of Computer Science, The University of Hong Kong.
Tu, C., Wang, W., Wang, J., 2002. Classifying the morphology of the nonsingular intersection curves of two quadric surfaces. In: Proceedings of Geometric Modeling and Processing. Tokyo, pp. 23–32.
Uhlig, F., 1976. A canonical form for a pair of real symmetric matrices that generate a nonsingular pencil. Linear Algebra Appl. 14, 189–209.
Walker, R., 1962. Algebraic Curves. Dover.
Wang, W., Goldman, R., Tu, C., 2003. Enhancing Levin's method for computing quadric-surface intersections. Comput. Aided Geom. Design 7, 401–422.
Wang, W., Joe, B., Goldman, R., 2002. Computing quadric surface intersections based on an analysis of plane cubic curves. Graph. Models 6, 335–367.
Wang, W., Krasauskas, R., 2004. Interference analysis of conics and quadrics. In: Goldman, R., Krasauskas, R. (Eds.), Topics in Algebraic Geometry and Geometric Modeling. In: Contemporary Mathematics, vol. 334. AMS, pp. 25–36.
Wang, W., Wang, J., Kim, M., 2001. An algebraic condition on the separation of two ellipsoids. Comput. Aided Geom. Design 18, 531–539.
Wilf, I., Manor, Y., 1993. Quadric-surface intersection curves: shape and structure. Comput.-Aided Design 10, 633–643.
Williamson, J., 1935. The equivalence of non-singular pencils of Hermitian matrices in an arbitrary field. Amer. J. Math. 57 (3), 475–490.
Yap, C., 2000. Fundamental Problems of Algorithmic Algebra. Oxford University Press, Inc.